Synthesis of Al_2O_3/AlN composite powders by plasma processed Al_2O_3 with various additives

F.Y.C. Boey, X.L. Zhao, and A.I.Y. Tok[a]
Nanyang Technological University, School of Materials Engineering, Singapore 639798, Singapore

A novel method was developed to produce Al_2O_3/AlN composite powders. The composite powders were synthesized by the direct nitridation of Al_2O_3 using various additives by plasma processed with two different types of gas (Ar/N_2 and N_2 plasma). The effects of these two different plasma gases and additives on the formation of the Al_2O_3/AlN composites were studied. The x-ray diffraction results in the composite powders showed that the cubic AlN was converted to the major phase while transient γ–Al_2O_3 was the minor phase when the composite powder was fully melted using nitrogen as the sole working gas. In contrast, the main phase was still α–Al_2O_3 when the composite powder was not well melted using the mixture of argon and nitrogen as the working gas. Carbon was found as an effective conversion additive to increase the cubic AlN of this composite powder up to 49 vol%. The reaction mechanism of forming this composite powder was also analyzed.

I. INTRODUCTION

Thermal plasma spraying techniques have been used for many years to produce layered coatings for many different applications.[1–3] Such coatings have been increasingly used in the automobile, aerospace, textile, biomedical, electrical, and optical industries to impart properties of wear resistance, thermal barrier, corrosion resistance, biocompatibility, and electrical insulation.[4–6] Although it was initially intended for coating purposes, plasma spraying has widened its scope to perform powder processing, which allows in situ production of ultrafine powders[7,8] and ceramic-matrix composite powders,[9] and opened up new approaches to material processing. Thermal spraying is characterized by its high temperatures (~10000 K), high specific energy densities, and high cooling rates.[10,11] The use of thermal spray methods to synthesize particulate systems in contrast has only been developed recently. Early attempts included the use of a direct current (dc) plasma reactor to form carbides from metal powders and gaseous precursors.[12] Fine SiC powders were also synthesized using SiO_2 particles and CH_4 gas in a dc plasma jet reactor.[13] Arc plasma methods were also used for the direct production of ultrafine silicon powers and nitrides/carbides of silicon, titanium, and tungsten.[14–16] Nanocrystalline zirconia powders were produced using zirconium butoxide solutions by thermal spray pyrolysis.[17] These recent works have demonstrated the feasibility of producing fine powders by reactive plasma spray processing, which is able to vary the extent of the chemical reaction in the plasma environment, allowing a reasonable method by which to prepare varying composite powder system. Composite materials have the ability to improve mechanical, chemical, and thermal behavior by combining materials with distinctive or supplementary properties.[18–20]

Recent works have shown how, using such a plasma spray method, a Al_2O_3/AlN integral composite powder system can be formed, which can be cost effectively sintered to give a pure AlN powders as well as monoclinic AlN substrate.[21,22] In the case of the latter, full densification of AlN was obtained below the sintering temperature of 1700 °C, avoiding the adverse formation of AlON and resulting in high thermal conductivity values. Many sintering aids have been identified for AlN,[23] among which alkaine earth metal[24] compound and yitrium and rare-earth metal[25] compounds are the most commonly studied. This paper presents a study on the preparation of a smaller Al_2O_3/AlN composite powder using plasma processing but with various additives. Ball-milled Al_2O_3 and different additives were used as the initial materials to prepare the Al_2O_3/AlN composites powders. The process characteristics and reaction mechanism of the composite powder were also studied.

II. EXPERIMENTAL PROCEDURE

Commercial Al_2O_3 powder (purity 99.6%) with an average particle size of 27 μm from Cerac, (Milwaukee, WI), was used as the starting material. Four different

[a]Address all correspondence to this author.
  e-mail: miytok@ntu.edu.sg

additives were investigated: activated carbon, CaF$_2$, Y$_2$O$_3$, and Sm$_2$O$_3$. Additive ratio was maintained at 10 wt% for all samples. The Al$_2$O$_3$ powder, together with each additive, was ball milled using a Fritsch (Laval, Canada) P-5 Planetary Mill with a 20:1 ball-to-weight ratio, at 200 rpm for 8 h. The particle size and its distribution of the powders were measured by a laser diffraction method using the Fritch Particle Sizer Analysette 22 (Germany). The average particle size of composite powders used for plasma processed was about 2.45 μm. After ball milling, the powders were plasma sprayed. Two different plasma atmospheres (Ar/N$_2$ and N$_2$) were investigated for all four types of samples. Figure 1 presents a schematic illustration of the apparatus used. This system consists of a plasma gun (GP-3, Prexair Technologies, Danbury, CT), a powder feed hopper (Miller Thermal, Danbury, CT), a vacuum reactor with cooling water, an exhaust gas treatment system and a reaction vacuum chamber for collecting the powders. The GP-3 spray gun, which was mounted at the front of a vacuum reactor, was operated at about 30 kW with either nitrogen gas or argon/nitrogen gas combinations. The powders were injected into the plasma arc using a vibration feeder by means of nitrogen gas and were directly nitrided. This process resulted in the formation of the composite powders. After collection from the vacuum reactor, the composite powders were kept dry in a desiccator.

Phase compositions of the Al$_2$O$_3$/AlN composite powders were determined by x-ray diffraction using Cu K$_\alpha$ radiation at 50 kV and 20 mA with a Philips (Allentown, NJ) MRD1880. All the peaks in the 2θ range from 20° to 80° were used to calculate the relative intensities.

To calculate the phase composition, the ratio of γ–Al$_2$O$_3$/(α–Al$_2$O$_3$ + γ–Al$_2$O$_3$) [Eq. (1)] and AlN/(γ–Al$_2$O$_3$ + AlN) [Eq. (2)] in the composition were expressed as:

$$R1 = \frac{I_{\gamma-Al_2O_3(400)}}{I_{\gamma-Al_2O_3(400)} + I_{\alpha-Al_2O_3(113)}} \quad , \quad (1)$$

$$R2 = \frac{I_{AlN(311)}}{I_{AlN(311)} + I_{\gamma-Al_2O_3(400)}} \quad , \quad (2)$$

where $I_{\alpha-Al_2O_3(113)}$, $I_{AlN(311)}$, and $I_{\gamma-A_2O_3(400)}$ were the integral intensity of the highest peak of α–Al$_2$O$_3$, cubic AlN, and γ–Al$_2$O$_3$, respectively.

The particle size and its distribution were measured by laser diffraction with a Fritch Particle Size Analysette 22. A scanning electron microscope (SEM) equipped with an energy-dispersive x-ray analyzer (EDX, Link 5130) was used for microstructural and elemental analysis. X-ray fluorescence (XRF) spectrometer (Philips, PW. 2400) was used to measure the element composition in the composite powders. The standard samples for XRF were made by mixing 3.5 g composite powder and 5 wt% wax. The samples were formed under 75 bar by Enerpac 15 Ton Press (Wellesley, MA) for 1 min. A Perkin-Elmer FT2000 Fourier transformed infrared spectroscopy (FTIR) was used to observe the Al-O and Al-N bonds in the composite powders produced. A Netzsch (Waldkraiburg, Germany) model DSC 404 differential scanning calorimeter was used to determine the powder reaction behavior with nitrogen up to 1550 °C at the heating speed of 5 °C/min.

III. RESULTS AND DISCUSSION

Figure 2 shows the XRD spectrum of the composite powder produced with Al$_2$O$_3$ and carbon, plasma sprayed using 30 kW in an argon/nitrogen atmosphere. It can be seen that α–Al$_2$O$_3$ was the dominant phase and that transient γ–Al$_2$O$_3$ also appeared in the composite powders. The ratio of γ–Al$_2$O$_3$ to α–Al$_2$O$_3$ was about 3:7 according to the Eq. (1). There was no evidence of AlN formation.

Figure 3 shows the XRD pattern of the same powder composition plasma processed using 30 kW in a nitrogen
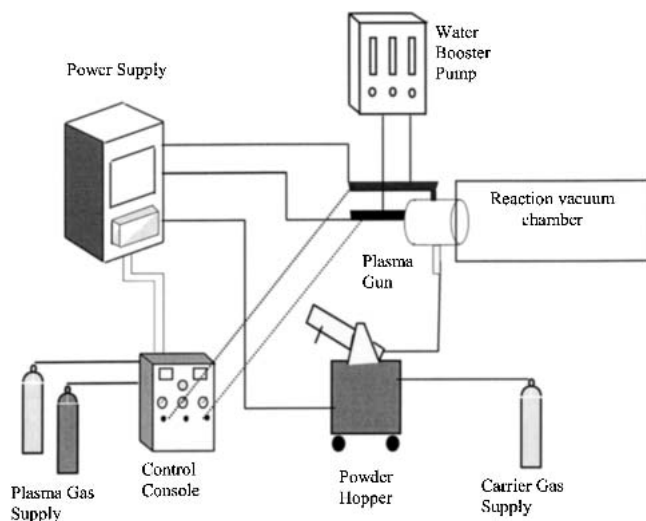

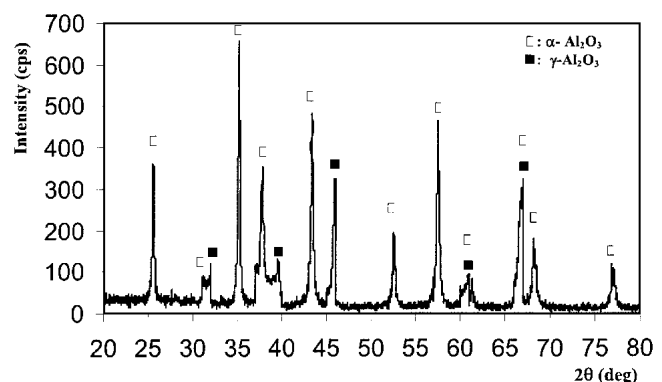FIG. 1. Schematic diagram of plasma processed system.

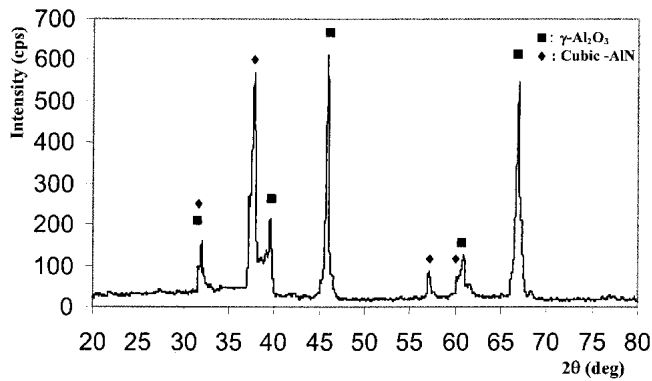FIG. 2. XRD pattern of plasma processed Al$_2$O$_3$/C powder in Ar/N$_2$ gas.

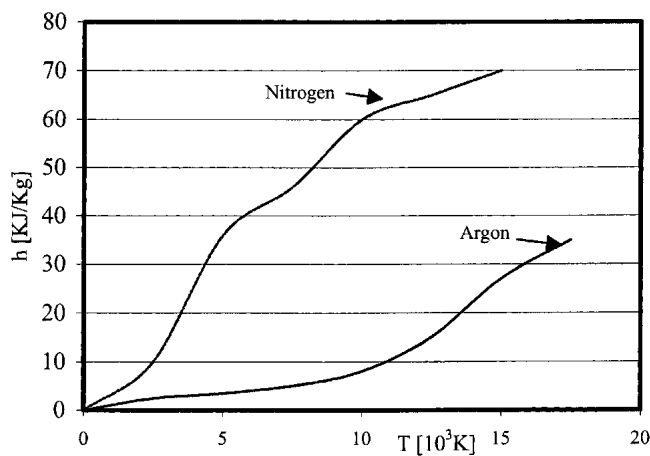FIG. 3. XRD pattern of plasma processed Al_2O_3/C powder in N_2 gas.

FIG. 4. Enthalpy of plasma gases.[26]

FIG. 6. SEM microstructure of plasma processed Al_2O_3/C powder in N_2 gas.
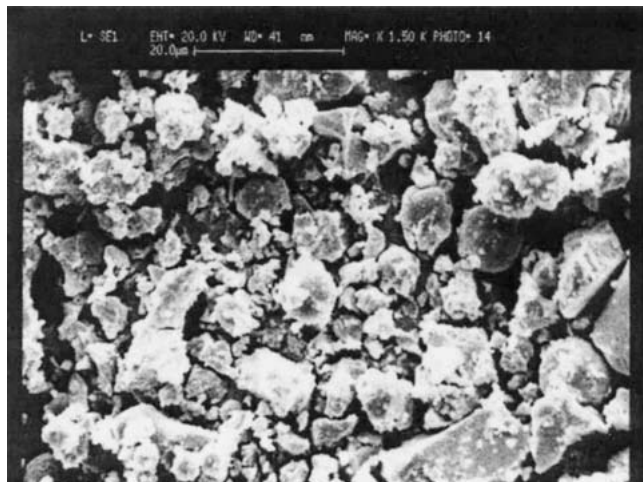

FIG. 5. SEM microstructure of plasma processed Al_2O_3/C powder in Ar/N_2 gas.

atmosphere. Evidently, all the original α–Al_2O_3 phase in the powder has converted to the transient γ–Al_2O_3. Figure 3 also shows the presence of cubic AlN in the resulting powders. The ratio of cubic of AlN to γ–Al_2O_3 calculated in Eq. (2) was about 1:1. It has been well
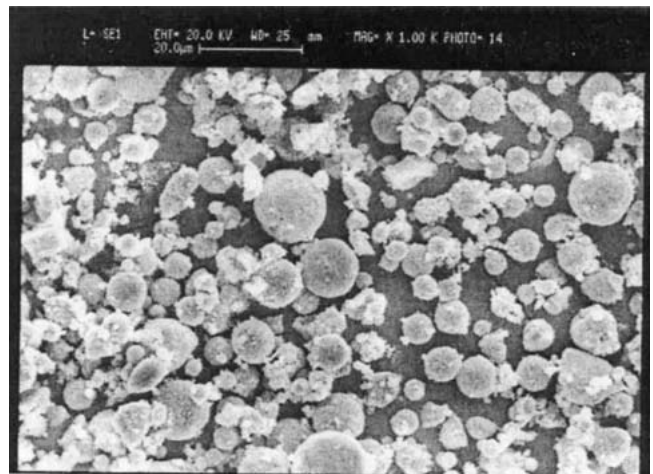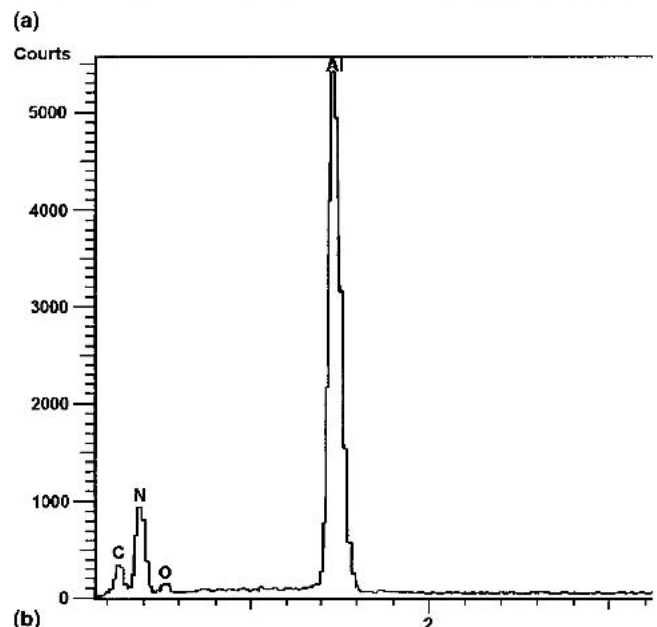
FIG. 7. (a) Surface microstructure and (b) EDX spectrum of plasma processed Al_2O_3/C powder in N_2 gas.

documented[26,27] that a dominant presented the meta-stable γ-alumina phase over the α-alumina phase confirms that the powders melted well. On the other hand, grains not fully melted would lead to the dominance of residual α-alumina. According to McPherson,[28] this formation is due to the lower energy for nucleation from liquid for γ than for α phase. The reason for the varying effect of different gases on particle melting is due to their different plasma heat enthalpy. It can be seen from Fig. 4 that nitrogen yielded a higher heat enthalpy than argon,[29] especially at higher temperatures, providing enough heat for complete particle melting.

It is known that AlN has a hexagonal crystalline form with a wurtzite-type structure, which is its most stable form. However, it can also exist as an oxygen-stabilized cubic structure, which is unstable at high temperatures in a nitrogen atmosphere.[30] In the plasma process using nitrogen as the plasma gas, AlN nuclei first forms on the surface of the molten Al$_2$O$_3$ particles and produces the cubic structure that contains nitrogen and oxygen ions. With the AlN nuclei growth in the nitrogen atmosphere, it gradually crystallizes to form a single-phase AlN hexagonal structure. Because of the high quenching rate of the plasma flame, there would not be enough time for the AlN to crystallize into its hexagonal form, thus forming

the oxygen-stabilizing cubic form during the high quench process. This led to the formation of oxygen-stabilized cubic AlN. However, this cubic AlN does not form when plasma is processed in an argon/nitrogen atmosphere. It is because the Al$_2$O$_3$ particles were not fully melted, and there is not enough nitrogen in the environment when the combined argon/nitrogen gas is used.

The evidence for a liquid-state reaction was seen in the change in morphology of the resulting plasma sprayed composite powder. Figures 5 and 6 show the SEM micrographs of the Al$_2$O$_3$/C powders plasma processed in argon/nitrogen plasma gas and nitrogen gas, respectively. It can be seen from Fig. 5 that the partially melted powders were irregularly shaped and coarse. In contrast, Fig. 6 shows fully spherical and individually densified powders after plasma processed. This shows conclusively that liquid state was achieved during the plasma reaction.

Figure 7(a) further shows a higher magnification of the spherical composite powders. The plasma processing resulted in a spherical particle with cracks on the surface, typical of rapidly cooled droplet-generated particles. The plasma processing resulted in a plasma flame above 10,000 K, generating extremely high heating and cooling rates to result in melting, reaction, evaporation, and
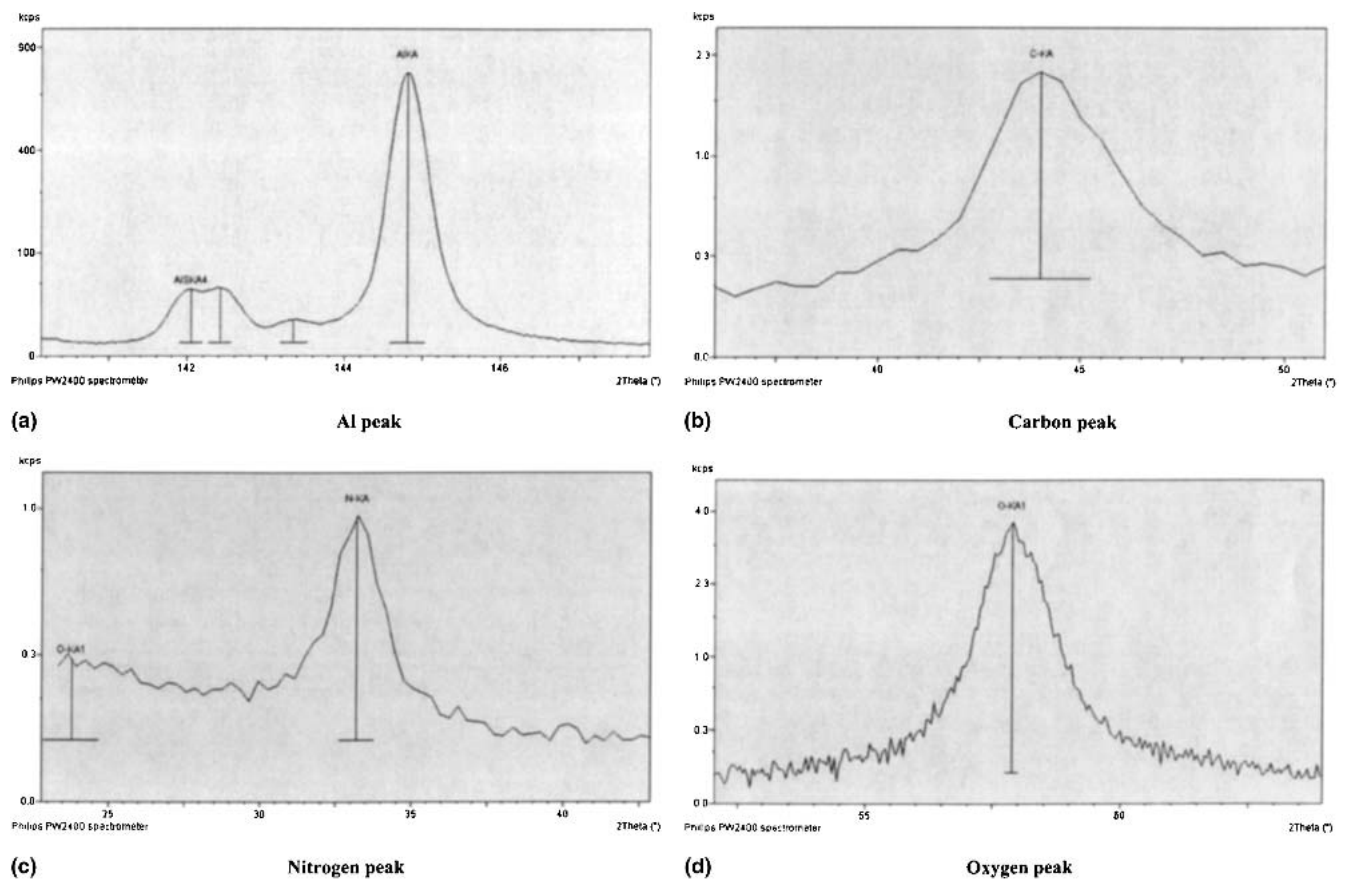

FIG. 8. XRF results of the composite powders.

cooling to solidification all within milliseconds. The rapid solidification process thus enabled the trace of crack formed on the spherical surface AlN also formed on the surface of the Al_2O_3 particles. This was identified by EDX, as shown in Fig. 7(b). The EDX results show the presence of elements of Al, C, N, and O. Because the elements of C, O, and N are low atomic number elements, further examination of the elements composition was measured by XRF (spectra shown in Fig. 8).

Figure 9 shows the FTIR spectroscopy results for the commercial Al_2O_3 and AlN as well as the composite powders. The infrared spectrum of the composite powders show two peaks related to the Al–N bond at around 750 and 1334 cm^{-1}, which confirm the presence of AlN. This result agrees with the EDX and XRF results. A strong Al–O bond was observed at 600 and 1636 cm^{-1}. The broad peak around 3400 cm^{-1} was the H–O bond due to the composite powders absorbing moisture of the air. Therefore, it is very important to keep the powders dry.
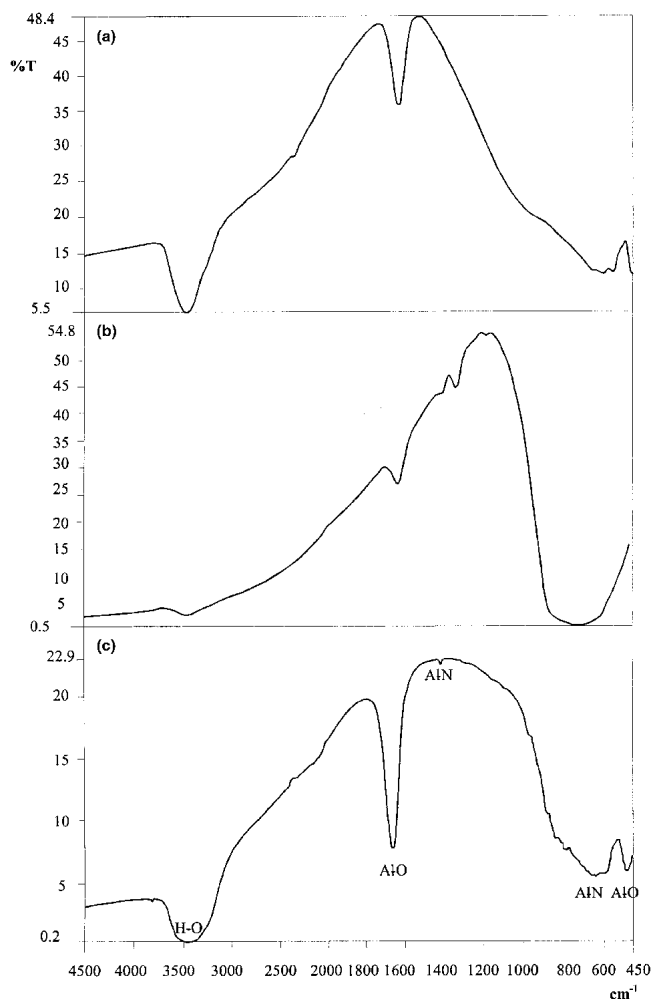
Figures 10 and 11 show the XRD spectrum plasma processed Al_2O_3 with and without Sm_2O_3, at 30 kW in nitrogen gas. As observed, the only $SmAlO_3$ phases are indicated in Fig. 10. The reaction equation for the formation of $SmAlO_3$ is as follows

$$Al_2O_3 + Sm_2O_3 = 2SmAlO_3 \quad . \tag{3}$$

It can also be seen that the amount of cubic AlN phase formed was nearly constant, with or without the addition of Sm_2O_3. Therefore, Sm_2O_3 was not an effective additive to synthesize Al_2O_3/AlN composite powders. Y_2O_3 and CaF_2 were also used as additives in the plasma processing. However, the results were similar, showing that these were also not effective additives to synthesize Al_2O_3/AlN composite powders.

Tables I and II list the phase composition and their relative volume ratio of plasma processed Al_2O_3 with different additives using the Ar/N₂ or N₂ plasma gas.

From Table II, carbon is certified as the only promoter for improving the content nitriding of Al_2O_3 in plasma processed. It is known[31] that Al_2O_3 was reduced by carbon by solid-solid mechanism in the processing of commercial carbothermal reduction of Al_2O_3, while the mechanism of AlN formation through the plasma processed of Al_2O_3 was different. The schematic models of
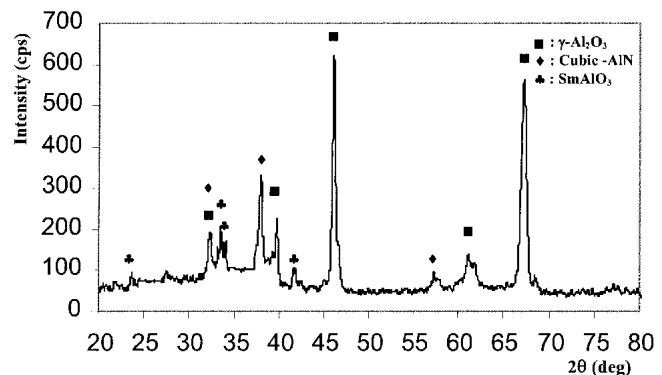
FIG. 9. FTIR spectra of: (a) commercial Al_2O_3, (b) AlN, and (c) plasma processed powders.

FIG. 10. XRD pattern of plasma processed Al_2O_3/Sm_2O_3 powder in N₂ gas.
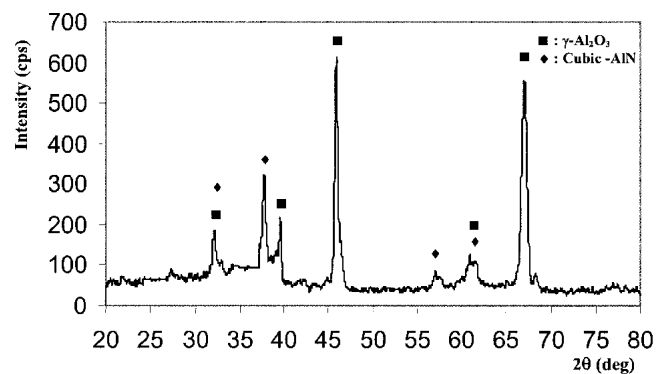
FIG. 11. XRD pattern of plasma processed Al_2O_3 powder in N₂ gas.

TABLE I. Phase composition of plasma processed Al$_2$O$_3$ with different additives using Ar/N$_2$ plasma gas.

Raw materials	Phase compositions after plasma processed (vol%)				
	γ–Al$_2$O$_3$	α–Al$_2$O$_3$	SmAlO$_3$	CaAl$_{10}$O$_{15}$F$_2$	Al$_5$Y$_3$O$_{12}$
Al$_2$O$_3$	30.4	69.6	0	0	0
Al$_2$O$_3$/C	30.8	69.2	0	0	0
Al$_2$O$_3$/Sm$_2$O$_3$	27.2	63.5	9.3	0	0
Al$_2$O$_3$/CaF$_2$	27.1	63.1	0	9.8	0
Al$_2$O$_3$/Y$_2$O$_3$	27.1	63.2	0	0	9.7

TABLE II. Phase composition of plasma processed Al$_2$O$_3$ with different additives using N$_2$ plasma gas.

Raw materials	Phase compositions after plasma processing (vol%)				
	Cubic-AlN	γ–Al$_2$O$_3$	SmAlO$_3$	CaAl$_{10}$O$_{15}$F$_2$	Al$_5$Y$_3$O$_{12}$
Al$_2$O$_3$	16.9	83.1	0	0	0
Al$_2$O$_3$/C	49.6	50.4	0	0	0
Al$_2$O$_3$/Sm$_2$O$_3$	8.1	82.7	9.2	0	0
Al$_2$O$_3$/CaF$_2$	8	82.2	0	9.8	0
Al$_2$O$_3$/Y$_2$O$_3$	12.1	77.8	0	0	9.1

these two processes were shown in Fig. 12. During the plasma process, liquid Al$_2$O$_3$ dissociated to Al and oxygen in the middle of flame due to high temperature. Al vapor was trapped rapidly by nitrogen over each Al$_2$O$_3$ particle. The reaction could have happened in the hot zone of flame and extended to the tunnel of the connector. The effects of carbon had two functions. First, it could be reacted with the oxygen in the vacuum chamber during the processing of plasma processed, in that the left nitrogen in the vacuum chamber had more chance to
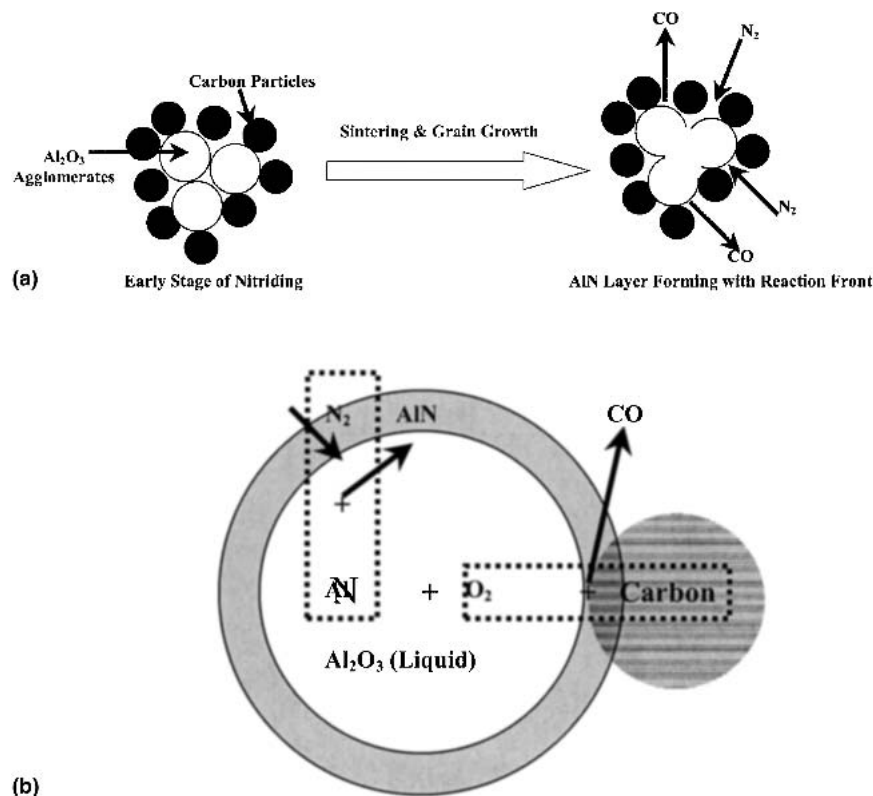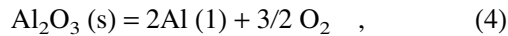

FIG. 12. Schematic models of the proposed reaction sequence with (a) carbothermal reduction of Al$_2$O$_3$ and (b) plasma processed of Al$_2$O$_3$ with carbon.

meet with Al vapor. Secondly, it also can be reacted with oxygen on the surface on the Al_2O_3 particle. The whole reaction is the solid–liquid–gas reaction mechanism where Al_2O_3 particle dissociating plays a determining role in the kinetics, which leads to the reaction mechanism through the following basic steps

$$Al_2O_3 \text{ (s)} = 2Al \text{ (1)} + 3/2 \, O_2 \quad , \qquad (4)$$

$$3C \text{ (s)} + 3/2 \, O_2 = 3CO \text{ (g)} \quad , \qquad (5)$$

$$2Al \text{ (l)} + N_2 = 2AlN \quad . \qquad (6)$$

While the addition of the additives except carbon did not result in a significant increase in the conversion extent to AlN, it is surmised that the process may be able to increase the reactivity of the plasma processed composite powders in being converted to AlN. To analyze this, both the starting powders of Al_2O_3/C/ Sm_2O_3 and the same powders after plasma processing were analyzed by a high temperature differential scanning calorimeter (DSC) to determine the reaction behavior in a nitrogen atmosphere.

Figure 13 shows the DSC results for Al_2O_3/C/Sm_2O_3 powders, before (curve 2) and after (curve 1) plasma processed using 30 kW in a nitrogen atmosphere. Curve 1 shows an exothermic peak, measuring about 24.3 J/g at 985 °C for the plasma processed powders. This represents the phase transformation of γ-Al_2O_3 into α-Al_2O_3:

$$\gamma\text{-}Al_2O_3 \rightarrow \alpha\text{-}Al_2O_3 \quad . \qquad (7)$$
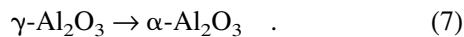
Additionally, a broad but comparatively small endothermic peak also appeared at about 1300 °C, measuring 568 J/g, which probably represents the nitriding reaction [as shown in Eq. (8)]. The DSC results for the unsprayed powders (curve 2), in contrast, show only one strong endothermic peak at about 1400 °C, measuring significantly higher at 5410 J/g, representing the extensively higher energy reaction of the powder. Evidently, the plasma spray process has conferred a higher reactivity to the

powders, resulting in a drastic reduction in the heat of reaction required from 5410 to 568 J/g.

$$Al_2O_3 + N_2 + 3CO = 2AlN + 3CO_2 \quad . \qquad (8)$$

IV. CONCLUSIONS

Al_2O_3/AlN composite powders were successfully produced by plasma processed Al_2O_3 with the activated carbon in nitrogen plasma. The results showed that plasma gas system and additives had a great influence on the phase composition of the Al_2O_3/AlN composite powders in the process of plasma processing. Starting α–Al_2O_3 was converted to transient γ–Al_2O_3 and cubic AlN when carbon additive was used, and plasma was sprayed in a nitrogen atmosphere. Activated carbon was as effective additive to increase the formation of cubic AlN. Maximum achievable cubic AlN content was about 49 vol%. EDX results further confirmed the presence of AlN in the composite powders. The morphology of the composite powders was spherical, with fine AlN particles formed on the surface of the Al_2O_3 particles.

REFERENCES

1. R. Suryanarayanan, Plasma Spray Applications for Electronic Materials, in *Plasma Spraying Theory and Application,* edited by R. Suryanarayanan (World Scientific Publishing, 1993), pp. 217–237.
2. E.D. Kubel, Plasma Spray Coatings of High YBaCuO Superconductors, *Adv. Mater. Proc.* **132,** 69 (1987).
3. S.L. Chen, Experimental Design and Optimization of Plasma-Sprayed Coatings, in *Thermal Spray Coatings,* edited by C.C. Berndt and T.F. Bernecki (ASM International, Materials Park, OH, 1993), pp. 95–127.
4. R.A. Miler and C.E. Lowell, Failure Mechanisms of Thermal Barrier Coatings Exposed to Elevated Temperatures, *Thin Solid Films,* **95,** 265 (1982).
5. D.J. Wortman, Properties of Plasma-Sprayed Bond Coats, *J. Mater. Sci. Eng. A* **121,** 437 (1989).
6. C.C. Koch, Materials Synthesis by Mechanical Alloying, *Int. Mater. Rev.* **33,** 201 (1988).
7. B. Kazuhiro, S. Nobuaki, and M. Yonezawa, Synthesis and Properties of Ultrafine AlN Powder by rf Plasma, *Appl. Phys. Lett.* **54,** 2309 (1989).
8. K. Ishizaki, T. Egashira, K. Tanaka, and P.B. Celis, Direct Production of Ultra-fine Nitride (Si_3N_4 and AlN) and Carbide (SiC, WC, and TiC) Powders by the Arc Plasma Method, *J. Mater. Sci.* **24,** 3553 (1989).
9. M.J. Koczak and M.K. Premkumar, Shaping and Forming of High Performance Powder Products, *JOM* **45,** 44 (1993).
10. C.C. Berndt and J.H. Yi, Composite Plasma Sprayed Coatings, in 12th International Thermal Spraying Conference, London, U.K., 1989; Paper 2.
11. S. Sampath and B. Gradnmndsson, Thermal Spray Research and Application, in *Proc. 3rd Nat. Thermal Spray Conf.,* edited by Thomas F. Bernecki (ASM International, Materials Park, OH, 1991), p. 357.
12. A.W. Weimer, *Carbide, Nitride, and Boride Materials: Synthesis and Processing* (Chapman & Hall, London, U.K., 1997), p. 246.
13. P.C. Kong and T.T. Huang, Synthesis of SiC powders using a DC plasma system, Proc. 6th Int. Symp. Plasma Chem. **1,** 219 (1983).
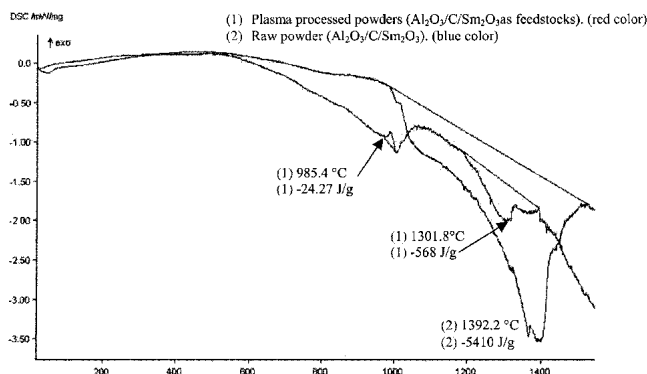
FIG. 13. DSC curves for plasma processed powders (1) and raw powder (2).

14. R.R. Tayler and S.A. Pizands, Plasma and Laser Processing of Materials, Proc. TSM 91 Annual Meeting, (Pergamon Press, Oxford, U.K., 1991), pp.123.

15. K. Tanaka and T. Egashira, Non-Oxide Materials: Applications and Engineering, *J. Mater. Sci.* **22,** 2192 (1987).

16. K. Ishizaki, T. Egashira, K. Tanaka, and P.B. Celis, Direct Production of Ultra-fine Nitride (Si_3N_4 and AlN) and Carbide (SiC, WC, and TiC) Powders by the Arc Plasma Method, *J. Mater. Sci.* **24,** 3553 (1989).

17. C.C. Berndt and J. Karthikeyan, Comparison of heat and momentum transfer to ceramic particles sprayed in Ar-H_2 and Ar-He plasma jets at atmospheric pressure, Proc. PEAM6, edited by C.C. Berndt and Ki Li (1987).

18. P.C. Nicholas, *Handbook of Ceramics and Composites* (1990), pp. 2–3.

19. H. Ishida, *Characterization of Composites Materials* (Butterworth-Heinemann, Boston, MA and Greenwich, CT, 1994), pp. 9–10.

20. T. Mah, Multicomponent Ceramic Powders, in *Chemical Processing of Ceramics,* edited by I. Lee (Bustrond, New York, 1994), pp. 75–105.

21. F.Y.C. Boey and L.M. Sun, High Dieletric Al_2O_3/AlN Composites Powder Using a Plasma Spray Approach for Microelectronics Application, *J. Mater. Sci.* **10,** 455 (1999).

22. F.Y.C. Boey, L. Cao, K.A. Khor, and A.I.Y. Tok, Phase Reaction and Sintering Behavior of an Al_2O_3–20 wt% AlN–5 wt% Y_2O_3 System, *Acta Mater.* **49,** 3117 (2001).

23. M. Billy, C. Devin, J. Jarrige, and J. Mexmain, Grain Growth in Annealed Aluminum Nitride, *Phys. Chem. Solid State* **32,** 381 (1984).

24. K. Komeya, H. Inoue, and A. Tsuge, Effect of Various Additives on Sintering of Aluminum Nitride, Yogyo-yokai-Shi, **89,** 330 (1982).

25. T.B. Jackson and A.V. Virkar, High Thermal Conductivity Aluminum Nitride Ceramics: The Effect of Thermodynamic, Kinetic, and Microtructural Factors, *J. Am. Ceram. Soc.* **80,** 1421 (1997).

26. P.A. Sieers, M.R. Jackson, R.L. Mehan, and J.R. Rairden, Production of Composite Structures by Low Pressure Plasma Deposition, *Ceram. Eng. Sci. Proc.* **6,** 896 (1985).

27. P. Boc, D. Fargeot, C. Gault, and F. Platon, Variations of the Elastic Moduli of Alumina During Structural Phase Transition, *Rev. Int. Hautes Temper. Refract.* **18,** 85 (1981).

28. R. McPherson, Formation of Metastable Phases in Flame and Plasma Prepared Alumina, *J. Mater. Sci.* **8,** 851 (1973).

29. E. Pfender, Fundamental Studies Associated With the Plasma Spray Process, in *Thermal Spray-Advances in Coating Technology* (Conference Proceedings), edited by D.L. Houck (ASM International, Materials Park, OH, 1988), pp. 1–10.

30. D. Ganguli and M. Chatterjee, Ceramic Powder Preparation: A Handbook (Kluer Academic Publishers, MA, USA, 1997), pp. 123-125.

31. Y. Baik, K. Shanker, J.R. Mcdermid, and A.L.D. Robin, Carbothermal Synthesis of Aluminum Nitride Using Sucrose, *J. Am. Ceram. Soc.* **77,** 2165 (1994).